Available online at www.sciencedirect.com
ScienceDirect
European Journal of Pharmaceutics and Biopharmaceutics 69 (2008) 94–105
European Journal of Pharmaceutics and Biopharmaceutics
www.elsevier.com/locate/ejpb

Research paper

Comparison of salmeterol xinafoate microparticle production by conventional and novel antisolvent crystallization

Darragh Murnane, Christopher Marriott, Gary P. Martin *

King's College London, Pharmaceutical Science Division, London, United Kingdom

Received 17 July 2007; accepted in revised form 21 September 2007
Available online 1 October 2007

Abstract

The production of microparticles for inhalation has relied on jet-milling while the potential for crystallization of microparticles has remained underexplored until relatively recently. Aqueous antisolvent crystallization of salmeterol xinafoate (SX) from poly(ethylene glycol) (PEG) and other organic (co)solvent systems was compared in order to evaluate factors determining the resultant microparticle properties. SX was crystallized by the addition of water to solutions of SX in PEG 400, PEG 6000, propan-2-ol, acetone and methanol. Crystalline particles were characterized by laser diffraction sizing, scanning electron microscopy and differential scanning calorimetry; PEG-media were characterized by viscometry. Crystallization of SX from PEG 400 produced crystals that exhibited a narrower size distribution than those crystallized from other conventional organic solvents. SX crystallized from PEG 6000 demonstrated a smaller median particle size ($D_{(v,0.5)} = 0.92 \pm 0.04$ μm) than PEG 400 crystallized SX ($D_{(v,0.5)} = 4.50 \pm 0.61$ μm). Crystals produced from PEG 400 (Span $= 2.49 \pm 0.10$) possessed a narrower particle size distribution (PSD) than those produced from PEG 6000 (Span $= 10.42 \pm 0.85$). SX crystals displayed a plate-like habit with growth limited to two dimensions irrespective of the initial solvent employed. The importance of the rate of generation of SX supersaturation on the PSD was determined using HPLC analysis. DSC showed PEG-crystallized SX to be free from metastable crystal phases in contrast to SX crystallized from propan-2-ol. Crystallization of SX from PEG was shown to follow classical nucleation theory and the crystallization method represents a viable alternative to the use of conventional solvents for the production of microparticles.

Keywords: Crystallization; Antisolvent micronization; Polymorphism; Poly(ethylene glycol); Salmeterol xinafoate; Microparticles

1. Introduction

In spite of the development of new engineering processes capable of generating powders for inhalation [1], crude crystallization followed by drying and comminution are the established and most extensively used techniques for their manufacture. The popularity of this approach has been attributed to the relative simplicity and ease of scale-up of such methods [2]. Micronization is an inefficient means of microparticle production resulting in highly cohesive and poorly flowing particles. Micronization can introduce solid state disorder into particles which affects formulation stability and can even be detrimental to dose availability from inhalation aerosols. An alternative strategy which has been proposed is that of solvent precipitation; a technique that can offer significant benefits in terms of control of the solid state compared to the traditional milling route [3,4].

A number of alternative constructive particle formation methods involving antisolvent crystallization have been proposed in the past decade. In all of these cases, the crystallization process necessitates the use of organic solvents for the crystallization of water-insoluble drugs. These techniques frequently require the use of various mixing

* Corresponding author. King's College London, Drug Delivery Research Group, Pharmaceutical Science Division, 150 Stamford Street, London SE1 9NH, United Kingdom. Tel.: +44 (0)20 7848 4791; fax: +44 (0)20 7848 4800.
E-mail address: gary.martin@kcl.ac.uk (G.P. Martin).

0939-6411/$ - see front matter © 2007 Elsevier B.V. All rights reserved.
doi:10.1016/j.ejpb.2007.09.016

technologies or crystal growth inhibitors to ensure the production of particles in the respirable size range (1–6 μm [5]). We have shown that it is possible to produce powders within this size range without the need for volatile organic solvents or stabilizers using conventional mixing techniques when poly(ethylene glycol) (PEG) is employed as the solvent in an aqueous-based antisolvent precipitation [6]. PEG is an attractive alternative to conventional solvents as it is environmentally benign and non-volatile [7], displays solubility in both water and non-polar solvents [8] and it efficiently solubilizes hydrophobic molecules [9]. PEG has been employed most frequently in the crystallization and recovery of proteins [10–12], but low molecular weight PEG has also been used as an antisolvent crystallization medium for low molecular weight pharmaceuticals [13].

It is highly desirable to understand and control the crystallization behaviour of compounds and this requires any link between the chemical and physical processes that influence nucleation and crystal growth to be established [14]. The solvent employed in a crystallization process can affect both the nucleation and growth phases of crystallization [15,16]. Hence the selection of the solvents used in the crystallization of an active pharmaceutical ingredient (API) can affect the polymorphic form and crystal habit (macromorphology) of the final crystal. Solvents of different polarity strongly affect the crystalline habit [17] and specific interactions such as hydrogen bonding can also affect crystal growth [18]. Cosolvents are by definition necessary for antisolvent crystallization, and their presence has been demonstrated to alter the growth of crystals from aqueous solutions [19].

PEG is a polymer with extensive capacity to form H-bonds and different crystal habits have been demonstrated by some authors when PEG was included in crystallization media [20,17], while other studies have not demonstrated any such effects [13]. Frequently reports of the effects of polymers on crystal growth fail to take into account the influence of such additives on the thermodynamic driving force for crystallization: supersaturation. Particle shape is affected by the kinetics of crystallization [21]. Nucleation kinetics are, in turn, also strongly affected by the choice of solvent, which determines the interfacial barrier between a crystal nucleus and the solvent.

Understanding the crystallization process from PEG/water antisolvent systems requires consideration of the hydrodynamic, kinetic and thermodynamic factors that affect it. The aim of this work was to examine the crystal habit and particle size distribution (PSD) of salmeterol xinafoate (SX) crystallized from a PEG solvent system. These crystals will be compared with those produced by crystallization from more conventional organic solvents.

2. Materials and methods

2.1. Materials

PEG 400, Analar® grade cyclohexane and HiPerSolv® grade ammonium acetate were purchased from BDH (VWR International Ltd., Poole, UK). High performance liquid chromatography grade methanol was purchased from Fisher Scientific Ltd. (Loughborough, UK) or from VWR International Ltd. Reagent grade acetone and propan-2-ol were purchased from Fisher Scientific Ltd. An Inertsil® ODS 2 column (5 μm, 200 × 4.6 mm i.d.) was obtained from Capital HPLC Ltd. (Broxburn, UK). PEG 6000 (Fluka BioChemika Ultra Grade) was purchased from Sigma–Aldrich Company Ltd. (Gillingham, UK). Nylon filters (0.45 μm pore size, 47 mm diameter) and cellulose acetate syringe filters (0.45 μm pore size, Schleicher and Schuell brand) were obtained from Whatman International Ltd. (Maidstone, UK). Plastic syringes were purchased from Becton and Dickinson (Oxford, UK). Water was produced by reverse osmosis using an ElgaStat unit (Elga LabWater, Marlow, UK). Silica gel was purchased from Prolabo (VWR International, UK). Salmeterol xinafoate (SX) was a generous gift from GlaxoSmithKline Pharmaceutical Development (Ware, UK).

2.2. Determination of equilibrium solubility

Solutions of 10% w/w or 5.5% w/w of either propan-2-ol or acetone or methanol were prepared in water. Additionally liquid mixtures of PEG 400 ($0\% < \text{PEG} < 100\%$ w/w) and PEG 6000 ($0\% < \text{PEG} < 60$ % w/w) with water were also prepared. Excess SX was added to a volume of each solution in a glass beaker and stirred using a high shear Silverson L4RT mixer (Silverson Machines Ltd., Chesham, UK). Aliquots of the suspensions were transferred to glass vials and sonicated for 40 min (Decon FS300B Bath, Decon Laboratories Ltd., Hove, UK). The samples were equilibrated for 72 h at 25 °C in a temperature controlled water bath (Grant SSD40, Grant Instruments, Chelmsford, UK) with the aid of magnetic stirring (H+P Labortechnik Ag., Oberschleissheim, Germany) Mixer. Samples were filtered (0.45 μm) or centrifuged at 16,060g for 5 min (Biofuge pico, Heraeus, Kendro Laboratory Products plc, Bishops Stortford, UK). The filtrates/supernatant were diluted accordingly and analyzed for drug content by high performance liquid chromatography (HPLC) according to a validated HPLC assay for SX [22]. Calculated solubilities of SX in water/PEG liquid mixtures were calculated from the regression equation of experimentally determined values of Log_{10} solubility as a function of PEG concentration (% w/w).

2.3. Rheology of PEG crystallization media

Solutions of PEG 6000 above 50% w/w were prepared by melting the polymer over a water bath at 65 °C and then adding water. The PEG 6000 solutions were used immediately and the others were placed in capped tubes which were then sealed with sealing film and stored in a refrigerator at 4 °C.

The kinematic viscosity, ν, ($\text{m}^2\,\text{s}^{-1}$) of PEG 400/water liquid mixtures was determined using a U-tube viscometer

according to the method of the European Pharmacopoeia (2007) using calibrated either size A, B, C, D or E U-tubes (Fisher Scientific Ltd.). Measurements were performed at 25.0 °C in a controlled temperature glass-sided water bath (Townson and Mercer Ltd., Manchester, UK), and solutions were allowed to equilibrate at 25.0 °C before measuring the flow times. The flow time of each solution was measured in triplicate or until 3 readings within 0.5 s had been obtained. The kinematic viscosity was converted to dynamic viscosity, η, (Pa s) according to Eq. (1):

$$v \times \rho = \eta \quad (1)$$

where ρ is the density of the PEG/water mixtures in kg m^{-3}, the values of which were obtained by conversion of the values of the density of PEG 400/water mixtures in g cm^{-3} as reported by Eliassi et al. [23].

The rheological properties of PEG 400/water and PEG 6000/water mixtures were studied using a Carri-Med CSL 100 Rheometer (TA Instruments Ltd., Crawley, UK) equipped with parallel plate measuring geometry according to the conditions detailed in Table 1. Rheometry was performed at 25 °C or 65 °C, which were achieved by use of the Peltier temperature controlled lower plate. Samples (~1 mL) were applied to the lower plate using a Gilson pipette with a modified tip (widened by removing a section equivalent to approximately 0.2 mL from the tip) to reduce effects of shear on the solutions/suspensions during application. The lower plate was then raised to create a predetermined gap between the plates. Rheograms of the aqueous solutions of PEG 400 and PEG 6000 were measured in triplicate. Dynamic viscosity was determined as the slope of a plot of shear stress as a function of the shear strain using TA Rheology Advantage software (version 5.1.42, TA Instruments Ltd.).

2.4. Crystallization of salmeterol xinafoate from cosolvent systems

2.4.1. Preparation of SX solutions

Solutions of SX in organic solvents were prepared by adding SX to volumetric flasks which had been weighed before and adding the appropriate solvent to a weight which would produce solutions of the required concentration. The flasks were then sealed with sealing film to avoid evaporation and sonicated briefly (Decon FS300B bath, Decon Laboratories Ltd., Hove, UK) until the drug was dissolved. Solutions of SX in PEG 400 were prepared using a method of high shear mixing. The appropriate amount of SX was weighed into a glass beaker and sufficient PEG 400 was added to achieve the required concentration of SX (% w/w). The beakers were covered with sealing film, and the solution was subjected to ultrasonication at 400 W and 40 kHz (for 5 min) to aid SX dispersion and dissolution. Thereafter the solutions were mixed using a Silverson L4RT Mixer with 1 tubular frame rod and a high shear square hole head according to the following protocol: 2000 rpm for 10 min, 3000 rpm for 10 min, 1000 rpm for 5 min and finally ultrasonication for 5 min to degas. The solutions were then filtered using a 0.45 μm cellulose acetate syringe filter into glass vials and sealed.

Solutions of SX in PEG 6000 were prepared initially as solids by a method of fusion mixing. PEG 6000 flakes were milled using a Retsch centrifugal mill (Glen Creston Ltd., Stanmore, UK). The particle size was not measured and appropriate quantities of SX and the PEG 6000 powder were blended so as to achieve the desired concentration of drug in PEG. Blending was achieved by placing the powders in glass vials possessing a volume three times greater than the powder blends. The vials were transferred to a Turbula Mixer (Glen Creston Ltd.) where mixing was effected for 35 min. The vials were transferred to a water bath maintained at 65 °C using a hot plate stirrer (RCD basic thermostat, IKA Werke GmbH and Co. KG, Staufen, Germany). The molten PEG and drug were mixed by stirring with a magnetic follower until they became visually clear, at which stage the heat was removed and the solutions were allowed to cool naturally to form solid solutions of the drug. Solid solutions were ground in a glass mortar and pestle to reduce the particle size but this was not measured.

2.4.2. Crystallization by antisolvent addition

The correct amount of drug solution was placed in a 250 mL glass beaker. Crystallization was achieved as described previously [6] by the addition of water as an antisolvent at an addition rate of 200 g min^{-1}, according to the experimental conditions which are shown in Table 2. In the case of PEG 6000 solutions, the solid solutions were allowed to melt on a water bath maintained at 65 °C with the beaker held in place under an overhead stirrer by means of a vertical retort clamp, until they became visually clear. The beaker was removed from the water bath as the addition of the antisolvent was commenced.

Samples (~1 mL; $n = 3$) were removed from the approximate midpoint of the crystallization liquor with a syringe 60–90 s after completing the addition of the antisolvent and once (~4 mL, $n = 3$) the crystallization process had been completed. The liquor was filtered through a 0.45 μm syringe filter into a volumetric flask (20 mL),

Table 1
Operating conditions for the rotational rheometric analysis of PEG/water liquid mixtures and crystallization media

Measurement system type	Parallel plate
Plate diameter	4.0 cm
Measurement system gap	250 μm
Measurement system inertia	1.510 μN ms^2
Equilibration time	60 s
Equilibration mode	Shear stress sweep
Start stress	0.010 Pa
End stress	5.000 Pa
Stress mode	Linear
Ascent time	60 s
Peak hold time	0 s
Descent time	60 s

Table 2
Experimental conditions employed for the antisolvent crystallization of salmeterol xinafoate

Crystallization experiment	Solvent	SX concentration (% w/w)	Ratio solution to antisolvent	Actual σ_{init}	Stirrer speed (rpm)	Final weight (g)	End time of crystallization (min)	Antisolvent addition
SX 1	PEG 400	0.67	8.56	2.14	400	110	30	Standard
SX 2	Acetone	1.50	9.06	2.08	400	110	30	Standard
SX 3	Methanol	0.79	8.79	2.12	400	110	30	Standard
SX 4	Propan-2-ol	1.06	9.03	2.08	400	110	30	Standard
SX 5	PEG 400	3.62	17.63	3.16	400	140	30	Standard
SX 6	Methanol	2.44	16.88	3.31	400	140	30	Standard
SX 7	PEG 400	3.99	11.23	3.51	900	170	20	Standard
SX 8	PEG 6000	4.00	11.15	3.48	900	170	20	Standard
SX A	PEG 400	1.72	8.87	2.58	400	120	30	Reverse
SX B	PEG 400	4.04	8.66	3.46	400	120	30	Reverse
SX C	PEG 400	5.00	17.95	3.52	400	120	30	Reverse
SX D	PEG 400	6.00	89.38	2.51	400	120	30	Reverse

weighed and then made up to volume for HPLC analysis of SX. The crystals were harvested by vacuum filtration using a 0.45 μm nylon membrane filter (47 mm diameter) housed in a glass filter unit (Millipore (UK) Ltd., Watford, UK). The wet cake was washed with 2×100 mL volumes of water; the latter having been filtered through a 0.45 μm nylon filter and pre-cooled to 4 °C. The washed filter cakes were transferred to Petri dishes, covered with perforated aluminium foil, and dried *in vacuo* at 50 °C overnight (Vacutherm, Heraeus GmbH, Hanau, Germany). The dry cake was transferred to sealed glass vials and stored at room temperature over dried silica gel in a glass desiccator. Where reported, crystal yields were determined as % theoretical yield according to (2):

$$\frac{\text{Actual yield(g)} \times 100}{\text{SX input(g)} - \text{SX in solution following crystallization(g)}} \quad (2)$$

2.4.3. Crystallization by reverse antisolvent crystallization

A weighed amount of water (140.00 g) was placed in a 250 mL glass beaker which was then positioned in the same configuration as for crystallization by standard antisolvent addition and stirring was initiated using the overhead stirrer. Drug solutions were weighed (to the nearest 0.001 g), filled into a 10 mL syringe, and introduced into the centre of the crystallization liquor at a rate of 60 g min^{-1}. The experimental conditions employed were as outlined in Table 2. The crystals were isolated as described above.

2.4.4. Recrystallization of micronized salmeterol xinafoate

A 1.6% w/v suspension of SX in propan-2-ol (110 mL) was prepared. This was transferred to a 250 mL round bottom flask, and purged with nitrogen gas. The suspension was heated at 60 °C on an oil bath placed on a magnetic stirrer hot plate to dissolve the SX. Crystallization was achieved by cooling with gentle stirring to 45 °C over two hours, followed by cooling to 37 °C under ambient conditions, at which temperature the solution was aged overnight. The suspension was then allowed to cool to 25 °C, at which temperature the crystalline suspension was allowed to age overnight, before finally being cooled to 21 °C, at which stage the crystals were harvested by filtration and drying as described above. The only change in the process was that the crystals were washed using 100 mL of SX-saturated propan-2-ol (4 °C) in place of water.

2.5. Calculation of supersaturation

The maximal supersaturation (σ_{init}) was calculated using Eq. (3):

$$\sigma_{init} = \ln \frac{c_s w_s}{w_{crys} s_{eq}} \quad (3)$$

where c_s is the concentration of drug in the solution, w_s is the mass of the solution taken, w_{crys} is the final weight of the crystallization medium and s_{eq} is the equilibrium solubility in the fully mixed cosolvent mixture. The maximal supersaturation therefore depends on the concentration of drug in the initial solvent, and the ratio of antisolvent to drug solution.

2.6. Characterization of the crystallized particles

The particle size distribution of SX microparticles was measured as previously reported by laser diffraction [6]. Microscopy was performed on prepared samples of SX powders using an FEI Quanta 200F field emission scanning electron microscope (FEI Company, Eindhoven, the Netherlands). Samples of SX powders were dispersed in cyclohexane in 5 mL stoppered glass vials, and sonicated briefly. Approximately 0.5 mL of the SX suspension was pipetted onto glass coverslips, which were adhered to microscope stubs with double-sided adhesive tape. The coverslips were coated with SX particles by removing the cyclohexane suspending solvent under vacuum at 50 °C (Vacutherm, Heraeus GmbH, Germany). The coverslips were then sputter coated with a layer of gold (Polaron

E51000, Polaron Equipment Ltd., UK). Thermographs were produced using a TA 2920 modulated differential scanning calorimeter (TA Instruments, UK). Approximately 1–2 mg of the test material was weighed accurately into 40 μL aluminium pans (TA Instruments, UK). Hermetically sealed pans were employed as both reference and sample pans. The instrument was calibrated according to the manufacturer's instructions for each heating rate using an indium standard. Samples were heated from 30 °C to 160 °C at 10 °C min^{-1}.

3. Results

3.1. Solubility of salmeterol xinafoate in cosolvent systems

The addition of all the solvents to water led to an increase in the solubility of SX in the crystallization liquor. The solubility of SX in various cosolvents used in the study is presented in Table 3. The lowest concentration of methanol employed (5.5% w/w) did not solubilize the drug relative to its aqueous solubility (51 ± 4 μg mL^{-1}). At the 10% w/w concentration of solvent, the solubilizing capacity of the solvent for SX was ranked *acetone* > *PEG* 400 > *propan-2-ol* > *methanol*. The determination of solubility allowed the crystallization of solutions at similar levels of supersaturation of SX in the crystallization medium regardless of the solvent chosen.

Both PEG 400 and PEG 6000 demonstrated a high solubilization capacity for SX. This was shown by the logarithmic increase in solubility of the drugs with increasing PEG content regardless of the molecular weight grade (Fig. 1). Plots indicated high linearity ($p < 0.001$ for both slope and intercepts) with correlation coefficients of 0.991 and 0.996 being obtained for PEG 400 and PEG 6000 curves, respectively. The regression equations for the solubility in the cosolvent systems were:

$$\mathrm{Log}_{10} S = 0.0335(\pm 0.0004)\mathrm{PEG400conc} + 1.736(\pm 0.022) \quad (4)$$

$$\mathrm{Log}_{10} S = 0.0351(\pm 0.0004)\mathrm{PEG6000conc} + 1.729(\pm 0.010) \quad (5)$$

Eqs. (4) and (5) enabled the calculation of SX solubility over the entire range of concentrations of PEG in the PEG/water liquid mixtures. Solubility of SX in aqueous PEG 6000 could not be determined at 25 °C above a concentration of 60% w/w PEG 6000 as such mixtures formed gels which could not be stirred effectively.

Table 3
Solubility of salmeterol xinafoate in solvent–water cosolvent systems of varying concentration (means ± SD, $n = 3$)

Concentration of cosolvent in water	Solubility of salmeterol xinafoate (μg mL^{-1})
10% w/w acetone	186 ± 24
10% w/w propan-2-ol	97 ± 1
10% w/w methanol	82 ± 3
10% w/w PEG 400	132 ± 6
5.0% w/w PEG 400 (calculated)	79 ± 1
5.5% w/w PEG 400	82 ± 3
5.5% w/w methanol	49 ± 2
8.0% w/w PEG 400 (calculated)	98 ± 1
8.0% w/w PEG 6000 (calculated)	101 ± 1

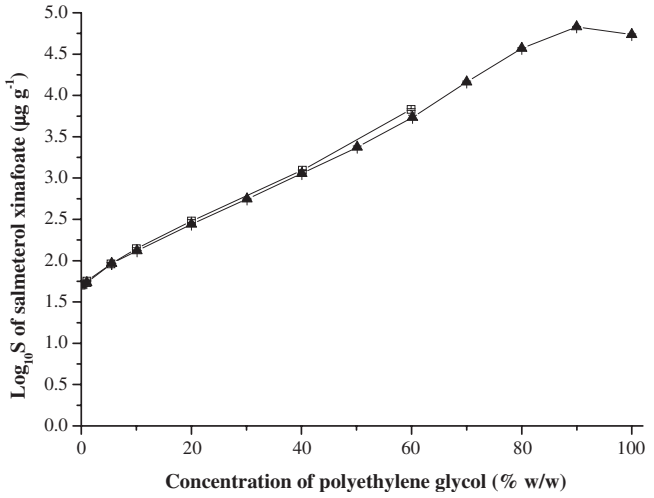

Fig. 1. The Log_{10} solubility (S) of salmeterol xinafoate as a function of the weight fraction of PEG 400 (▲) and PEG 6000 (□) in water at 25 °C (data points represent means ± SD, $n \geqslant 3$).

3.2. Rheological assessment of PEG crystallization solutions

A plot of the logarithm of dynamic viscosity as a function of PEG 400 concentration measured by U-tube viscometry demonstrated linearity (see Fig. 2). There was some suggestion of a plateau being attained at high concentrations of PEG (>90% w/w). This plot also demonstrates the similarity of the viscosity determined by the rotational rheometer and constant shear U-tube viscometer. Although the two lines have different slopes and intercepts, they exhibit very similar shapes, indicating that the rotational rheometer may be used to study changes in the

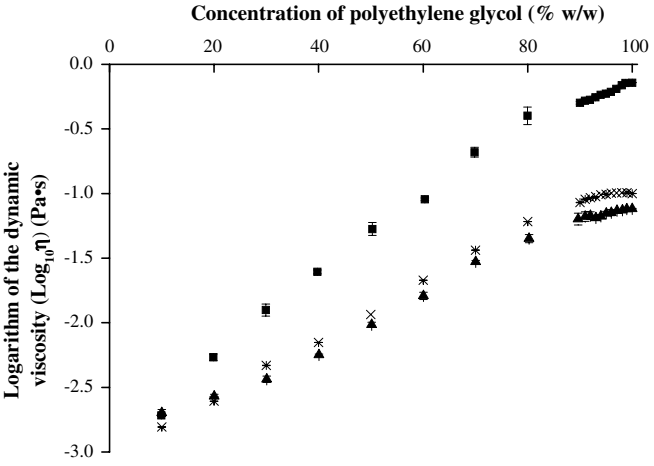

Fig. 2. Plot of the logarithm of dynamic viscosity as a function of weight concentration determined by rotational rheometry of aqueous PEG 6000 (■) solutions at 65 °C, PEG 400 (▲) solutions at 25 °C; and of aqueous PEG 400 solutions (×) determined by U-tube viscometer (means ± SD, $n = 3$).

viscosity of solutions as a function of PEG concentration. This was desirable to allow reasonable analysis times when high concentrations of solid grade PEG were employed.

Also presented in Fig. 2 is a plot of dynamic viscosity as a function of concentration of PEG 6000 at 65 °C. This demonstrates that solutions of PEG 6000 have a greater dynamic viscosity except at the lowest concentration studied of 10% w/w PEG. The slope of the plots of viscosity of PEG 400/water and PEG 6000/water mixtures appeared to decrease at higher concentrations of PEG. Nevertheless, linear regression was shown to be relevant with a correlation coefficient of greater than 0.986. It is clear from the plots that even at the higher temperature employed (65 °C), PEG 6000/water mixtures have a greater viscosity than PEG 400/water mixtures. The intercepts should be identical (i.e., the viscosity of water) for the U-tube and rotational results for PEG 400/water mixtures (-2.970 ± 0.019 and -2.938 ± 0.019 Pa s, respectively). The difference obtained using the two techniques is most likely a result of the skewing attributable to the plateau region and its contribution to the significant lack of fit ($p < 0.05$) of the line at the terminal regions of both plots.

3.3. Antisolvent crystallization of salmeterol xinafoate

3.3.1. Particle size distribution

The particle size distributions along with the % yields of the SX crystals formed by antisolvent crystallization are shown in Table 4. There was a significant difference in the 10% cumulative undersize diameter between SX crystallized from different solvents (ANOVA, $p < 0.001$). The SX crystals derived from acetone solution were found to have a lower $D_{(v,0.1)}$ value than those obtained by crystallization from methanol or PEG 400 ($p < 0.05$, Tukey's test) but not those crystallized from propan-2-ol. SX crystallized from either propan-2-ol or PEG 400 cosolvents resulted in batches having significantly smaller $D_{(v,0.1)}$ than those crystallized from methanol. Crystals precipitated from acetone demonstrated a larger median diameter ($p < 0.05$) than those crystallized from the other three solvents. There was, however, no difference in the median diameter of crystals obtained in the latter three batches. Finally, the following trend was seen for the cumulative 90% undersize diameter of crystals produced from the different solvents (ANOVA and Tukey's test, ($p < 0.05$):

acetone > propan-2-ol > PEG 400 = methanol.

A Student's *t*-test showed that the microcrystals produced at a higher supersaturation level from a methanol solution were significantly larger than those from PEG 400 (SX 6 and SX 5, respectively). A Student's *t*-test demonstrated that the 10% cumulative undersize and the median diameter of crystals produced from PEG 6000 (SX 8) were significantly smaller ($p < 0.001$) than those produced from PEG 400 (SX 7) under identical conditions. There was, however, no significant difference in the cumulative 90% undersize diameter ($p = 0.066$), demonstrating the wider particle size distribution of crystals produced from the higher molecular weight polymer. This finding was also evident from the calculation of the span ($(D_{(v,\ 0.9)} - D_{(v,0.1)})/D_{(v,0.5)}$) of the PSD ($2.49 \pm 0.10$ and 10.42 ± 0.85 ($n = 5$) for SX 7 and SX 8, respectively).

HPLC analysis of the crystallization media was performed to determine the degree of supersaturation of the media following addition of the antisolvent. The details are presented in Table 5. There was no significant difference between supersaturation levels 1.5 min after addition of the aqueous antisolvent ($p = 0.071$) to any of the solutions at comparable levels of σ_{init}. Significant differences were observed between solutions in the supersaturation at the crystallization endpoint, 30 min after addition of the antisolvent ($p = 0.018$). The supersaturation in the acetone-containing system (SX 2) was significantly larger than that in the methanol-containing system (SX 3), but not that in either the PEG 400 (SX 1) or propan-2-ol (SX 4) systems. There was no significant difference between the

Table 5
The initial supersaturation (σ_{init}) of salmeterol xinafoate in the crystallization media and the supersaturation (σ) at varying stages during crystallization (1.5 min and upon termination at 30 min, except * at 20 min) (means ± SD of 3 filtered samples from each crystallization batch)

Experiment	Solvent	σ_{init}	$\sigma_{1.5\ \text{min}}$	σ_{terminal}
SX 1	PEG 400	2.14	1.91± 0.14	0.26 ± 0.10
SX 2	Acetone	2.08	1.68 ± 0.11	0.34 ± 0.10
SX 3	Methanol	2.12	1.97 ± 0.04	0.15 ± 0.03
SX 4	Propan-2-ol	2.08	1.95 ± 0.16	0.20 ± 0.03
SX 5	PEG 400	3.16	1.93 ± 0.01	0.10 ± 0.03
SX 6	Methanol	3.31	2.30 ± 0.01	0.30 ± 0.22
SX 7*	PEG 400	3.51	2.11 ± 0.02	0.36 ± 0.03
SX 8*	PEG 6000	3.48	1.36 ± 0.16	0.70 ± 0.01

Table 4
Particle size distribution of salmeterol xinafoate crystals produced by standard antisolvent crystallization from comparative solvents (means ± SD, $n = 5$)

Experiment	Solvent	σ_{init}	$D_{(v,0.1)}$ (μm)	$D_{(v,0.5)}$ (μm)	$D_{(v,0.9)}$ (μm)	Yield (%)
SX 1	PEG 400	2.14	1.28 ± 0.11	7.29 ± 0.40	15.23 ± 0.73	65.4
SX 2	Acetone	2.08	0.84 ± 0.04	11.03 ± 1.49	26.96 ± 1.25	86.7
SX 3	Methanol	2.12	1.98 ± 0.24	7.76 ± 0.42	16.00 ± 0.80	66.9
SX 4	Propan-2-ol	2.08	1.02 ± 0.02	8.48 ± 0.36	19.65 ± 0.77	67.9
SX 5	PEG 400	3.16	0.70 ± 0.01	3.59 ± 0.10	9.33 ± 0.21	39.8
SX 6	Methanol	3.31	0.97 ± 0.08	4.95 ± 0.30	11.19 ± 0.35	n/d
SX 7	PEG 400	3.51	0.71 ± 0.02	4.50 ± 0.61	11.84 ± 1.11	77.3
SX 8	PEG 6000	3.48	0.55 ± 0.01	0.92 ± 0.04	10.12 ± 1.15	79.5

crystallization media comprising methanol, PEG 400 and propan-2-ol.

The supersaturation of the methanol medium (SX 6) was significantly higher at 1.5 min but not at termination of crystallization than the solution in PEG 400 from which SX was crystallized at the same level of supersaturation (SX 5). The supersaturation after 1.5 min in the PEG 6000 medium (SX 8) was significantly smaller than that in the equivalent PEG 400 medium (SX 7) ($p = 0.02$), while the reverse situation was the case at termination of crystallization (20 min).

3.3.2. Crystal morphology

Examination of scanning electron micrographs of the particles (Fig. 3) indicated that the growth of all crystals produced by antisolvent micronization was limited to two dimensions, since plate-like crystals were produced. The crystals produced by antisolvent crystallization were thinner and more flaky than the micronized material used as the starting material. Crystals produced from acetone appeared as fused agglomerates of many smaller particles, which provides an explanation for the larger median diameter and broader particle size distribution when measured

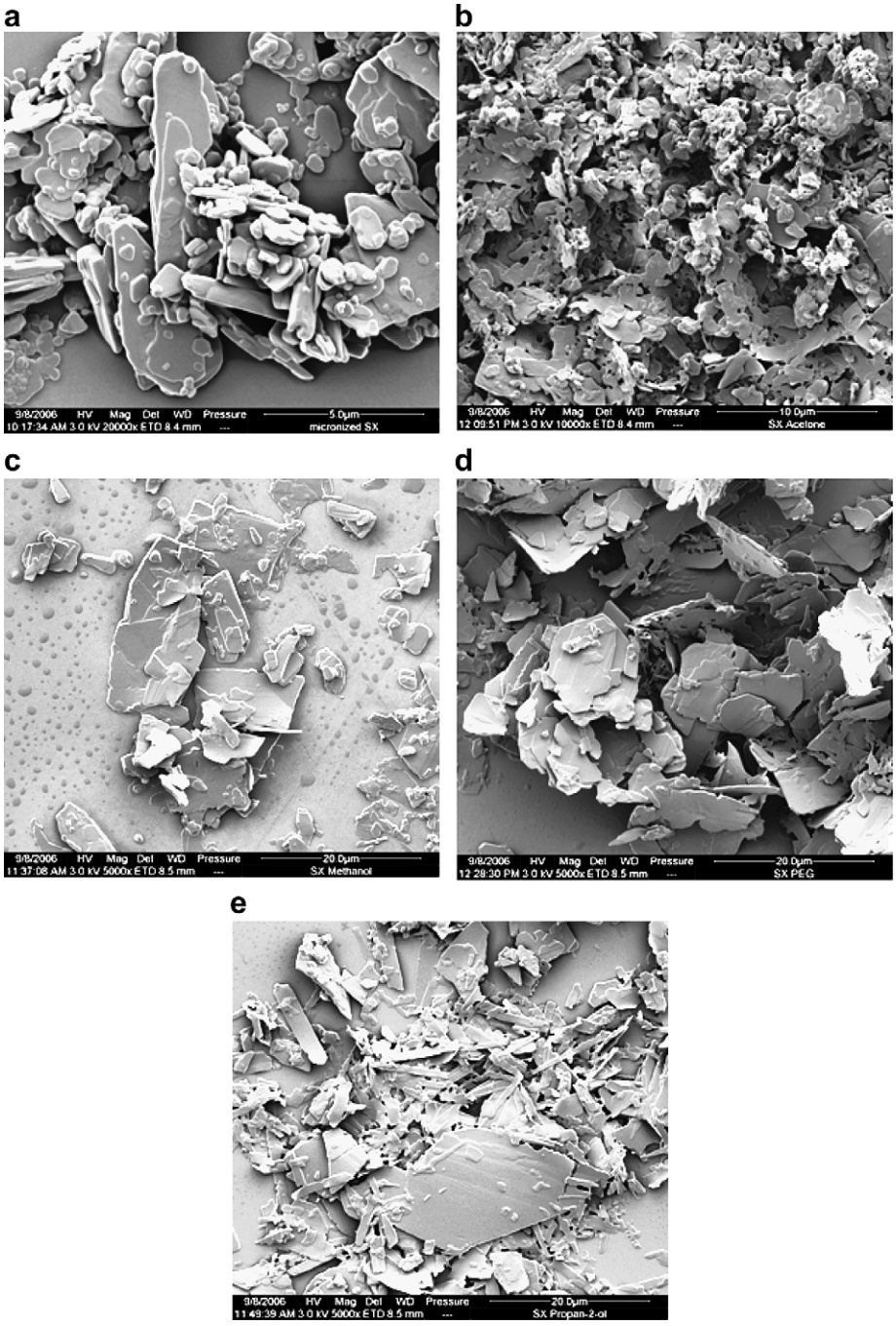

Fig. 3. Scanning electron micrographs of: micronized salmeterol xinafoate used as starting material (a); salmeterol xinafoate crystallized by antisolvent addition from acetone (b); methanol (c); polyethylene glycol 400 (d) and propan-2-ol (e).

by laser diffraction. Larger plate-like crystals of SX crystallized from acetone were also visible. Further morphological differences were observed in crystals obtained from propan-2-ol, with many appearing with reduced diameters, as rods.

3.3.3. Thermodynamic factors controlling crystallization from PEG 400

Table 6 presents the particle size distributions and % yields of SX crystals isolated 20 min after reverse antisolvent crystallization (stirrer speed of 400 rpm) of SX in PEG 400 solutions at two nominal supersaturation levels of $\sigma_{init} = 2.6$ and $\sigma_{init} = 3.5$, with varying PEG concentration in the crystallization medium. ANOVA ($p < 0.001$) revealed significant differences in both the cumulative 10% undersize and median diameters, between the samples. Tukey's test, when applied, revealed that crystals produced at similar supersaturation levels displayed similar diameters, i.e. (SX A = SX D) < (SX B = SX C). For the cumulative 90% undersize diameter the following relationship was seen at the 5% significance level: SX A = SX C = SX D, while SX A > SX B and SX B < SX D. This demonstrates that for systems containing the same concentration of PEG in the crystallization medium (SX A and SX B), there was a decrease in median particle diameter by increasing the supersaturation. However, it was also seen that the same particle size was produced by generating the same level of supersaturation, with a lower concentration of PEG in the crystallization medium.

3.4. Salmeterol xinafoate polymorphism

The differential scanning thermographs (Fig. 4) revealed the improved polymorphic purity of SX crystallized from PEG solvents compared to the commercial micronized material (mSX) and mSX which was recrystallized by slow cooling from propan-2-ol. This was apparent from the absence of the recrystallization exotherm and the melting endotherm of the SX II enantiotropic polymorph following the melting of the SX I enantiotrope at 122 °C.

4. Discussion

The solvents used in the antisolvent crystallization of SX were all demonstrated to solubilize the molecule to different

Table 6
Particle size distribution (means ± SD, $n = 5$) of salmeterol xinafoate crystallized by reverse antisolvent addition of PEG 400 solutions to water at different PEG concentrations and different levels of drug supersaturation (σ_{init})

Experiment	PEG content (% w/w)	σ_{init}	$D_{(v,\ 0.1)}$ (μm)	$D_{(v,\ 0.5)}$ (μm)	$D_{(v,0.9)}$ (μm)	Yield (%)
SX A	9.96	2.58	0.94 ± 0.08	5.42 ± 0.64	12.08 ± 1.26	69.3
SX B	9.93	3.46	0.79 ± 0.08	3.85 ± 0.87	9.22 ± 1.94	73.8
SX C	5.01	3.52	0.73 ± 0.02	4.16 ± 0.19	10.55 ± 0.18	56.1
SX D	1.04	2.51	0.99 ± 0.03	5.29 ± 0.19	11.39 ± 0.39	56.7

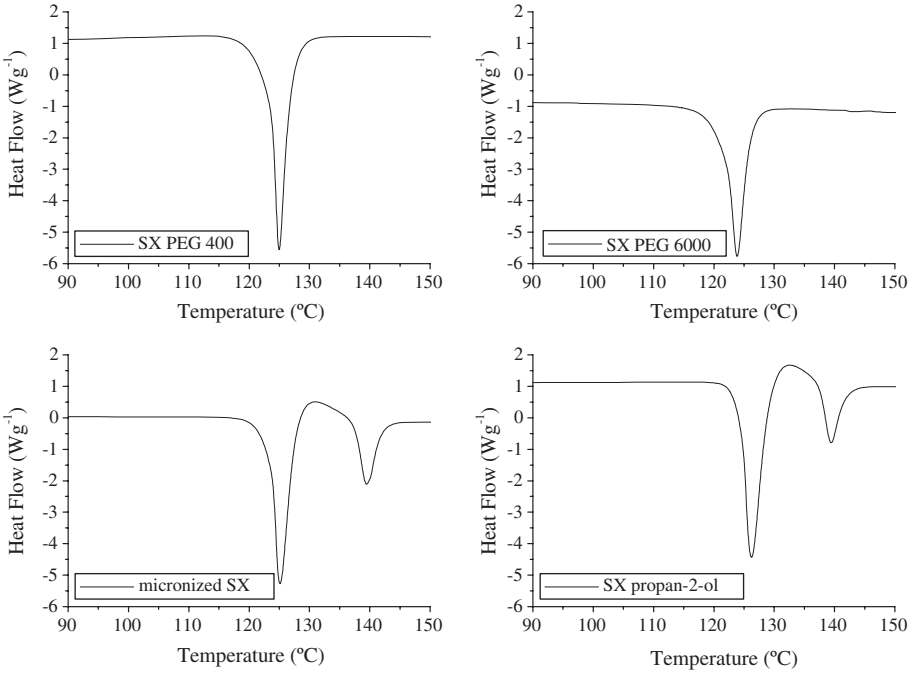

Fig. 4. Differential scanning calorimetry thermographs of salmeterol xinafoate (SX) crystallized from PEG 400 and PEG 6000 by aqueous antisolvent crystallization, micronized SX and SX recrystallized from propan-2-ol.

extents at the 10% w/w level (Table 3). The weight fraction solubilization curves for PEG 6000 and PEG 400 liquid mixtures with water were similar (Fig. 1). Solubilization by PEG is achieved when PEG molecules disrupt the water lattice [24] with individual ethylene oxide units behaving as a small molecular weight solute when interacting with water [25]. Ethoxyl oxygen groups may be considered to be water-structure breakers because they can accept H-bonds from the water molecules. Hydroxyl oxygen groups (i.e., alcohol termini of the PEG molecules) can also donate H-bonds to water and enhance water structure [26].

Due to the solubilities differing from cosolvent system to cosolvent system, it was necessary to employ different concentrations of SX in the respective solvents to achieve the same level of supersaturation in the crystallization medium. Supersaturation and its process of generation are the key determinants of the thermodynamic driving force for crystallization. Their effects must also be considered when studying the effect of additives and crystallization solvents on crystal properties. Supersaturation was calculated assuming instantaneous molecular mixing of the solution and antisolvent without simultaneous crystallization (σ_{init}, Eq. (3)).

SX precipitated from the different solvents varied in their particle size distributions (Table 4), with the broadest PSDs seen in crystals produced from propan-2-ol and acetone. The lowest median particle diameter was produced when PEG 6000 was used as the solvent. It is of note that the crystallization of SX from methanol and PEG 400 produced similar particle size distributions, although when the supersaturation level was increased further, crystals from PEG 400 were smaller. SEM analysis demonstrated the presence of a limited number of large particles which had undergone a growth phase when SX was crystallized from PEG 400 (Fig. 3d). The similarity of the median diameters regardless of crystallization solvent and the SEM analysis suggest that PEG did not serve as a crystal growth inhibitor in the traditional sense as suggested previously [27]. Instead PEG served as an alternative solvent suitable for antisolvent crystallization, capable of producing microparticles of SX. The crystal yields were highly encouraging (ranged from 56.1 to 86.7%) although all crystallization processes were performed at the laboratory scale.

The limitation of SX growth to two dimensions leading to plate-like crystals has been noted previously [28]. The crystals produced by antisolvent crystallization were thinner and more flaky than the micronized material used as the starting material, a feature which was noted for SX produced by supercritical fluid precipitation [29]. The plate-like morphology may arise from an inhibition of growth on the slowest growing crystal face due to solvent interactions or to kinetic phenomena arising from the rapid rate of crystallization during antisolvent crystallization. A mixture of morphologies was evident for SX crystallized from acetone with plates and fused agglomerates of many smaller crystals (Fig. 3b). Such perikinetic agglomeration is a common means of evolution of the PSD during antisolvent precipitation experiments [30].

The largest decrease in the supersaturation 1.5 min after addition of the antisolvent was seen for acetone–water crystallizations (Table 5) and it is interesting that this batch of crystals also corresponded to the crystals with the widest particle size distribution, and the smallest $D_{(v,0.1)}$ values. A period of extensive desupersaturation occurred therefore between 1.5 min and the termination of crystallization (after 30 min), which allowed crystal growth to occur for all solvent systems. There was some evidence of incorporation of smaller particles into the growth faces of the larger crystals in the case of SX precipitated from propan-2-ol (Fig. 3e). A similar phenomenon attributed to secondary nucleation was noted in the crystallization of lactose monohydrate produced by antisolvent crystallization [31].

The crystallization system involving PEG 400 does appear to reach homogeneity of SX concentration as quickly as conventional solvents, as seen by the similar desupersaturation profile to both methanol and propan-2-ol. This is in contrast to previous reports of antisolvent crystallization processes involving PEG solutions not achieving a good state of mixing and phase separation occurring [32]. In antisolvent crystallization the actual supersaturation is determined by the competing processes of solution–antisolvent mixing and nucleation [33]. Thus the supersaturation predicted by Eq. (3) is never usually achieved. The profile of generation of supersaturation is crucial in determining the PSD and depends on the efficiency of mixing and whether localized supersaturation prevails more in one solvent than another, leading to increased nucleation [30]. The second factor is the slope of the solubilization curve, as this determines the generation and extent of the supersaturation. This is conceivably different from cosolvent to cosolvent system. Despite the identical supersaturation at 1.5 min in some systems, there is no clear indication how the previous supersaturation profile may have peaked during the addition of antisolvent, or how this supersaturation was dissipated.

The use of high molecular weight PEG grades is not immediately obvious as a solvent system for crystallization, and previous reports of PEG as a crystallizing solvent utilized low molecular weight grades [13]. Molten PEG-2000 has been reported as a reaction solvent allowing a rapid kinetic rate [7]. The particle size distribution obtained for SX crystallized using PEG 6000 (Table 4) offers an interesting comparison to that obtained with PEG 400, because the solubilization curves for both cosolvents are similar. The dramatically smaller median particle size produced by crystallization from molten PEG 6000 is indicative of a very high nucleation rate (note the greater desupersaturation within 1.5 min). In order to exploit PEG as a solvent for crystallization, it was necessary to consider the macroviscosity of the polymeric solvents (resistance to flow). This is because solvent viscosity affects the fluid dynamics (and hence solution mixing [34]) which are crucial for the

generation of supersaturation, as well as the diffusion of solute during crystal growth [30].

Precipitation is a process initiated at the molecular level. It depends on the dispersion and mixing of solvents on different scales to generate supersaturation. Micromixing is the process of molecular diffusion and engulfment of regions of different solvent composition below the Kolmogorov microscale [34] and results in the generation of supersaturation. Mesomixing is the large-scale mass transfer of a solution and is also known as turbulent mixing [35] and can result in localization of supersaturation. Macromixing occurs on the scale of the crystallizer and conveys a region of fluid where micro- and mesomixing is occurring through regions of varying turbulence.

It has been demonstrated that an instantaneous interfacial tension exists between viscous miscible solvents [36] and that the mixing of viscous solutions is likely to lead to a segregation on the mesoscale [37]. Viscosity also affects the timescale of micromixing which leads to effects on the particle diameter following precipitation [38]. Micromixing is affected when diffusion of the water antisolvent molecules is impaired by the microviscous environment which exists in dissolving PEG [39,40] whilst solute diffusion will also be slower in the viscous polymeric solvent. Microviscosity is the resistance to molecular motion and flow. The high viscosity of PEG at all stages of antisolvent addition (note the logarithmic scale in Fig. 2) is expected, therefore, to affect the balance of the mixing scales responsible for generating localized or generalized supersaturation. The poorer mixing with PEG solvents can result in a greater degree of local supersaturation, leading to a large number of small nuclei. A localized peaking of supersaturation resulting in a higher rate of nucleation is consistent with the smaller median diameter which resulted when SX was crystallized by addition of water to the more viscous PEG 6000 molten solution compared to PEG 400 (Table 4).

Only small differences existed between the median diameters of SX crystallized from propan-2-ol, methanol, acetone and PEG 400 at the same level of supersaturation (Table 4). It was reported that at low supersaturations (applicable to the latter four batches) when the nucleation rate is low PSD is essentially independent of mixing phenomena [41]. The tailing of the particle size distribution represented by the high $D_{(v,0.9)}$ with PEG 6000 value demonstrates that PEG was not behaving as a traditional crystal growth inhibitor. Lower supersaturation existed in PEG 6000 than PEG 400 solutions at 1.5 min. Thus the following period of desupersaturation was less likely to result in further nucleation in the PEG 6000 liquor than in PEG 400 allowing the opportunity for particle growth. Additionally the higher viscosity barrier to molecular diffusion provided by PEG 6000 relative to PEG 400 at the crystal–solution interface may not limit crystal growth because as relative supersaturation drops below approximately 10, crystal growth ceases to be purely diffusion controlled [42].

The main thermodynamic driving force for crystallization is the actual supersaturation of the drug [43]. By considering Table 6, it is apparent that the PEG antisolvent crystallization system obeys classical nucleation theory which states the lowest median particle size is achieved with the highest possible supersaturation [43] due to increased rates of primary nucleation [42]. It is interesting that the crystal size distribution and the median crystal diameter was affected more by the supersaturation, than by the concentration of PEG 400 in the crystallization medium (Table 6). This suggests either that PEG 400 is functioning only as a crystallizing solvent requiring mixing, or that any specific effects of PEG upon crystallization require a critical concentration, which was exceeded in all cases.

SX is currently produced commercially by crystallization from a hot solution in propan-2-ol, which is quench cooled by addition to cooled propan-2-ol [28]. This process results in macrocrystals which must be micronized by jet-milling to generate particles of a size suitable for inhalation therapy. The particles produced by antisolvent micronization from PEG solvents were shown to possess a particle size distribution within the 1–10 μm size range as measured by laser diffraction, and hence may be useful for localized pulmonary drug delivery.

SX has been reported to exhibit enantiotropic polymorphism [44], with the form I polymorph (SX I) being most stable at room temperature. SX crystallized from propan-2-ol demonstrates two major endothermic events. These are the melting of SX I at ~125 °C which is followed by an exothermic re-crystallization, while the second endotherm corresponds to the melting of the form II polymorph (SX II) at ~139 °C [28]. Since milling can induce a solid state transition between polymorphic forms of drug substances [45], the potential for enantiotropic transformation of SX as it is micronized for inhalational purposes requires some consideration. The recrystallization of SX II has been attributed to the presence of nuclei of SX II within the predominantly SX I lattice [46] and the crystallinity of SX has also been shown to be damaged by the micronization process [4].

Crystallization of SX from PEG solvents by a rapid precipitation process at high supersaturation resulted in crystals which displayed no conversion to SX II from the melt upon heating (Fig. 4). The absence of recrystallization and melting of form II SX has been attributed to freedom from metastable form II seeds produced as result of concomitant crystallization or conversion upon milling [46]. It is interesting that SX crystallized slowly from propan-2-ol demonstrated recrystallization of SX II from the melt (Fig. 4). It was previously suggested that aggressive quench crystallization of SX led to crystal disordering [4] that was increased upon milling (for production of mSX). However, in the current study it has been shown that lattice disorder or concomitant crystallization may be inherent in a propan-2-ol crystallization process, because aggressive crystallization from PEG solvents did not lead to the production of detectable metastable crystal

phases. SX crystallized from PEG solvents displayed freedom from the presence of metastable regions (crystallites of SX II within the lattice). As such crystallization from PEG solvents represents an improvement over the current method of production of micronized SX in that the material is produced as the thermodynamically stable form at room temperature.

5. Conclusions

Crystallization of SX from PEG solvents demonstrated similar behaviour to crystallization from conventional solvents. Classical models of nucleation could be applied to PEG antisolvent micronization as shown by the dependence of the particle size distribution and nucleation rate on supersaturation. It was also shown that high molecular weight grades of PEG can be used as solvents for the crystallization of small molecular weight drugs. The control of the particle size distribution appeared to be mediated by the process of generation of supersaturation and the period of nucleation upon mixing the solution and the aqueous antisolvent. Finally the production of SX microcrystals by an antisolvent micronization process employing PEG solvents resulted in particles demonstrating improved solid state properties compared to micronized material. Microparticles of SX produced by aqueous crystallization from PEG possess potential for application in topical inhalation therapy.

Acknowledgements

The authors are grateful to MedPharm Ltd. and King's College London for financial support.

References

[1] A.H.L. Chow, H.H.Y. Tong, P. Chattopadhyay, B.Y. Shekunov, Particle engineering for pulmonary drug delivery, Pharm. Res. 24 (2007) 411–437.
[2] H. Schiavone, S. Palakodaty, A. Clark, P. York, S.T. Tzannis, Evaluation of SCF-engineered particle-based lactose blends in passive dry powder inhalers, Int. J. Pharm. 281 (2004) 55–66.
[3] H. Steckel, N. Rasenack, P. Villax, B.W. Muller, In vitro characterization of jet-milled and in-situ-micronized fluticasone-17-propionate, Int. J. Pharm. 258 (2003) 65–75.
[4] B.Y. Shekunov, J.C. Feeley, A.H.L. Chow, H.H.Y. Tong, P. York, Physical properties of supercritically processed and micronised powders for respiratory drug delivery, "KONA" Powder Science and Technology in Japan (2002) 178–187.
[5] J.N. Pritchard, The influence of lung deposition on clinical response, J. Aerosol Med. 14 (2001) S19–S26.
[6] D. Murnane, The crystallization and characterization of particles for the delivery of inhaled drugs (Ph.D. thesis), King's College London, University of London, 2007.
[7] J. Chen, S.K. Spear, J.G. Huddleston, R.D. Rogers, Polyethylene glycol and solutions of polyethylene glycol as green reaction media, Green Chem. 7 (2005) 64–82.
[8] J.M. Harris, in: J.M. Harris (Ed.), Introduction to Biotechnical and Biomedical Applications of Poly(ethylene glycol), Plenum Press, New York, 1992, pp. 1–14.
[9] E. Rytting, K.A. Lentz, X.Q. Chen, F. Qian, S. Venkatesh, Aqueous and cosolvent solubility data for drug-like organic compounds, AAPS J. 7 (2005) E78–E105.
[10] M. Rito-Palomares, Practical application of aqueous two-phase partition to process development for the recovery of biological products, J. Chromatogr. B 807 (2004) 3–11.
[11] V.K. Sharma, D.S. Kalonia, Polyethylene glycol-induced precipitation of interferon alpha-2a followed by vacuum drying: development of a novel process for obtaining a dry, stable powder, AAPS Pharm. Sci. 6 (2004).
[12] T. Arakawa, S.N. Timasheff, Mechanism of poly(ethylene glycol) interaction with proteins, Biochemistry (Mosc) 24 (1985) 6756–6762.
[13] X. Wang, C.S. Ponder, D.J. Kirwan, Low molecular weight poly(ethylene glycol) as an environmentally benign solvent for pharmaceutical crystallization and precipitation, Crys. Growth Des. 5 (2005) 85–92.
[14] S.L. Morissette, O. Almarsson, M.L. Peterson, J.F. Remenar, M.J. Read, A.V. Lemmo, S. Ellis, M.J. Cima, C.R. Gardner, High-throughput crystallization: polymorphs, salts, co-crystals and solvates of pharmaceutical solids, Adv. Drug Del. Rev. 56 (2004) 275–300.
[15] N. Blagden, R.J. Davey, Polymorph selection: challenges for the future? Crys. Growth Des. 3 (2003) 873–885.
[16] M. Lahav, L. Leiserowitz, The effect of solvent on crystal growth and morphology, Chem. Eng. Sci. 56 (2001) 2245–2253.
[17] R. Adhiyaman, S.K. Basu, Crystal modification of dipyridamole using different solvents and crystallization conditions, Int. J. Pharm. 321 (2006) 27–34.
[18] H. Wen, K.R. Morris, K. Park, Hydrogen bonding interactions between adsorbed polymer molecules and crystal surface of acetaminophen, J. Colloid Interface Sci. 290 (2005) 325–335.
[19] L.J.W. Shimon, M. Vaida, L. Addadi, M. Lahav, L. Leiserowitz, Molecular recognition at the solid–solution interface – a relay mechanism for the effect of solvent on crystal-growth and dissolution, J. Am. Chem. Soc. 112 (1990) 6215–6220.
[20] A. Nokhodchi, N. Bolourtchian, R. Dinarvand, Dissolution and mechanical behaviors of recrystallized carbamazepine from alcohol solution in the presence of additives, J. Cryst. Growth 274 (2005) 573–584.
[21] S. Piana, M. Reyhani, J.D. Gale, Simulating micrometre-scale crystal growth from solution, Nature 438 (2005) 70–73.
[22] D. Murnane, G.P. Martin, C. Marriott, Validation of a reverse-phase high performance liquid chromatographic method for concurrent assay of a weak base (salmeterol xinafoate) and a pharmacologically active steroid (fluticasone propionate), J. Pharm. Biomed. Anal. 40 (2006) 1149–1154.
[23] A. Eliassi, H. Modarress, Densities of poly(ethylene glycol) plus water mixtures in the 298.15–328.15 K temperature range, J. Chem. Eng. Data 43 (1998) 719–721.
[24] D. Sailaja, K.N. Raju, G.S.S. Devi, K. Subbarangaiah, Ultrasonic behaviour of aqueous solutions of polyethylene glycols on the temperature of adiabatic compressibility minimum of water, Eur. Polym. J. 34 (1998) 887–890.
[25] M.J. Hey, D.P. Jackson, Attenuated total reflection FT-IR study of hydrogen bonding in water/ether mixtures, Chem. Phys. Lett. 309 (1999) 69–74.
[26] J.J. Max, C. Chapados, Infrared spectroscopy of acetone–methanol liquid mixtures: hydrogen bond network, J. Chem. Phys. 122 (2005) 14504.
[27] S.L. Raghavan, A. Trividic, A.F. Davis, J. Hadgraft, Crystallization of hydrocortisone acetate: influence of polymers, Int. J. Pharm. 212 (2001) 213–221.
[28] S. Beach, D. Latham, C. Sidgwick, M. Hanna, P. York, Control of the physical form of salmeterol xinofoate, Org. Process Res. Dev. 3 (1999) 370–376.
[29] B.Y. Shekunov, J.C. Feeley, A.H.L. Chow, H.H.Y. Tong, P. York, Aerosolisation behaviour of micronised and supercritically processed powders, J. Aerosol Sci. 34 (2003) 553–568.
[30] J. Franke, A. Mersmann, The influence of the operational conditions on the precipitation process, Chem. Eng. Sci. 50 (1995) 1737–1753.

[31] H. Larhrib, G.P. Martin, D. Prime, C. Marriott, Characterisation and deposition studies of engineered lactose crystals with potential for use as a carrier for aerosolised salbutamol sulfate from dry powder inhalers, Eur. J. Pharm. Sci. 19 (2003) 211–221.
[32] X. Wang, J.M. Gillian, D.J. Kirwan, Quasi-emulsion precipitation of pharmaceuticals. 1. Conditions for formation and crystal nucleation and growth behavior, Crys. Growth Des. 6 (2006) 2214–2227.
[33] M. Aoun, E. Plasari, R. David, J. Villermaux, A simultaneous determination of nucleation and growth rates from batch spontaneous precipitation, Chem. Eng. Sci. 54 (1999) 1161–1180.
[34] J. Baldyga, J.R. Bourne, S.J. Hearn, Interaction between chemical reactions and mixing on various scales, Chem. Eng. Sci. 52 (1997) 457–466.
[35] B. Shekunov, J. Baldyga, P. York, Particle formation by mixing with supercritical antisolvent at high Reynolds numbers, Chem. Eng. Sci. 56 (2001) 2421–2433.
[36] S.E. May, J.V. Maher, Capillary-wave relaxation for a meniscus between miscible liquids, Phys. Rev. Lett. 67 (1991) 2013–2016.
[37] J. Baldyga, J.R. Bourne, R.V. Gholap, The influence of viscosity on mixing in jet reactors, Chem. Eng. Sci. 50 (1995) 1877–1880.
[38] J.F. Chen, C. Zheng, G.T. Chen, Interaction of macro- and micromixing on particle size distribution in reactive precipitation, Chem. Eng. Sci. 51 (1996) 1957–1966.
[39] S.L. Laporte, A. Harianawala, R.H. Bogner, The application of malononitriles as microviscosity probes in pharmaceutical systems, Pharm. Res. 12 (1995) 380–386.
[40] R.H. Bogner, S.L. Laporte, B.M. Hartz, D.L. Albanese, M. Bradley, Experimental evidence for the development of a microviscous layer near the surface of dissolving polyethylene glycol, Int. J. Pharm. 151 (1997) 155–164.
[41] J. Baldyga, L. Makowski, W. Orciuch, Interaction between mixing, chemical reactions, and precipitation, Ind. Eng. Chem. Res. 44 (2005) 5342–5352.
[42] A. Mersmann, Crystallization and precipitation, Chem. Eng. Proc. 38 (1999) 345–353.
[43] N. Rodriguez-Hornedo, D. Murphy, Significance of controlling crystallization mechanisms and kinetics in pharmaceutical systems, J. Pharm. Sci. 88 (1999) 651–660.
[44] H.H. Tong, B.Y. Shekunov, P. York, A.H. Chow, Characterization of two polymorphs of salmeterol xinafoate crystallized from supercritical fluids, Pharm. Res. 18 (2001) 852–858.
[45] H.G. Brittain, Effects of mechanical processing on phase composition, J. Pharm. Sci. 91 (2002) 1573–1580.
[46] H.H.Y. Tong, B.Y. Shekunov, P. York, A.H.L. Chow, Thermal analysis of trace levels of polymorphic impurity in salmeterol xinafoate samples, Pharm. Res. 20 (2003) 1423–1429.